Egyptian Knowledge Bank
https://ijmti.journals.ekb.eg/

International Journal of
Materials Technology and Innovation
Volume 4, Issue 2 (2024), pages 1-8

Online ISSN 2682-4299

Failure Analysis of a Fuel Supply Tube of an Aircraft Engine

Mohamed Wahba*, Khalid M. Hafez, Abdel-Monem Elbatahgy

Central Metallurgical Research and Development Institute, Helwan, Cairo 11421, Egypt

* Corresponding author: E-mail: ma_wahba@yahoo.com

Received……30 Sep. 2024
Accepted……17 Oct. 2024
Published……31 Dec. 2024

Abstract

This paper presents a failure analysis of a fractured fuel supply tube and its associated assembly clip from an aircraft engine. The assembly clip, made of 17-7 PH stainless steel, exhibited fracture initiation at the inner surface of its terminal hole. Chemical analysis showed conformity to standard material specifications, and microstructural examination revealed a tempered martensite matrix. Scanning electron microscopy identified radial fatigue marks and evidence of fretting fatigue, transitioning to brittle fracture near the crack's termination. The fuel tube failed near the butt-welded joint, with no surface defects detected by dye penetrant testing. Chemical analysis confirmed the material met specifications for type 347 stainless steel. Microstructural analysis showed fracture initiation in the heat-affected zone, with low-cycle fatigue and grain boundary cracking observed. Scanning electron microscopy revealed fatigue striations and a transition to brittle fracture near the outer surface, indicating a combined fatigue and brittle failure mechanism. This investigation highlights the role of fatigue in both the fuel tube and clip failures, providing insights into improving component durability in aerospace applications.

Keywords: Fuel tube failure, Fretting fatigue, Heat-affected zone

1. Introduction

The structural integrity of fuel systems in aircraft is of principal importance, as their failure can lead to catastrophic consequences. Fuel tubes are subjected to various mechanical and environmental stresses during operation. Significant thermal fluctuations, pressure variations, and vibrations make these tubes susceptible to different types of failures including fatigue, corrosion, and creep [1, 2]. Understanding the mechanisms that lead to the failure of these critical components is essential for improving design, maintenance, and safety in aerospace applications.

Fatigue fractures are among the most prevalent forms of failure in aircraft fuel tubes, due to the cyclic nature of the stresses they experience during flight [3]. Even though the original design of the fuel tubes and the materials selected for their fabrication typically possess good fatigue resistance, problems often arise when defects are introduced during manufacturing or installation. Such defects can significantly reduce the fatigue life of a component, leading to premature failure under normal operating conditions. A prime example of fatigue failure was documented in an augmenter assembly fuel tube, where an investigation revealed that the tube had failed due to fatigue cracking [1]. In this case, residual stresses introduced during the installation process, particularly from the forces applied during mounting, created a favorable environment for fatigue cracks to initiate and propagate. These stresses, not originally accounted for in the design, resulted in the premature failure of the tubes. Similarly, the presence of manufacturing defects can negatively affect the fatigue strength of fuel tubes. M. Nazir et al. [4] analyzed the fatigue failure of a leaking fuel tube and found that welding defects such as lack of fusion, played a key role in the initiation of fatigue cracks by acting as stress concentration sites. Another case [5] involved the afterburner fuel manifold of a jet engine, where defective welding techniques resulted in the concentration of stress at the welded joints leading to the initiation of fatigue cracks. In addition to

IJMTI vol. 4 issue 2 (2024) 1-8 https://doi.org/ 10.21608/IJMTI.2024.325019.1108

mechanical fatigue, thermal fatigue has also been identified as a significant failure mechanism in aircraft fuel tubes. M. Mansoor et al. [6] reported the occurrence of thermal fatigue cracks in fuel spray tubes, which were subjected to severe thermal cycling during operation. Detailed analysis revealed that sharp angles in the weld regions acted as stress raisers, amplifying the thermal stresses experienced during each cycle. These stress concentrations promoted the initiation and growth of fatigue cracks, which eventually led to the failure of the tubes.

Another commonly encountered fatigue failure mechanism in aero-engines is fretting fatigue [7]. This usually takes place at the interface of contacting bodies subjected to oscillatory forces, which induce small-scale relative displacements. The contact surface typically exhibits slip regions, where relative motion takes place. This displacement leads to surface degradation and heat generation due to frictional energy dissipation [8]. Fretting fatigue involves two distinct regimes: the gross slip regime and the partial slip regime [9]. The first regime is characterized by high slip amplitudes resulting in the generation of wear debris, a condition referred to as fretting wear. Conversely, at low slip amplitudes in the partial slip regime wear is minimal and fretting fatigue becomes the dominant mechanism [10]. It has been reported that a 50-70% reduction in fatigue strength is caused by fretting [11]. One example of the impact of fretting conditions on the failure of aircraft engines was reported in [12], where the investigations indicated that faiulre of the aircraft spline shaft made of 15-5 PH stainless steel was attributed to diminshed fatigue strength by fretting fatigue.

This article aims to provide a comprehensive failure analysis of an aircraft fuel tube, and its associated assembly clip focusing on the interaction between operational stresses, material properties, and manufacturing-induced defects.

2. Background

While cruising at an altitude of 28,000 feet, the aircraft's monitoring systems triggered a second-level alert, indicating a lateral fuel imbalance. Specifically, the left wing's fuel tank showed an 800 kg difference compared to the right wing. As the aircraft began landing, smoke was observed emanating from the right engine. After touching down and during the landing roll, the situation escalated when the right engine caught fire. The fire caused significant damage to the engine, its cowling, and the tail cone of the aircraft. Fortunately, no injuries were reported among the passengers or the crew.

The engine in question had undergone routine maintenance just two weeks prior to the incident, which included a standard visual inspection of all tubes, referred to as "Inspection A." This inspection is mandated every 450 flight hours as part of regular preventive maintenance. The purpose of this procedure is to identify potential wear, leaks, or damage to fuel lines and other critical components. Details of the engine's operational history before the subject flight are provided in Table 1.

An onsite inspection of the damaged engine was conducted by personnel from the Central Directorate of Aircraft Accident Investigation (CDAAI). The inspection revealed key details about the assembly and fixation mechanisms used for electrical cables, hydraulic lines, and fuel tubes. Typically, these components are secured to the engine body using clips and bolts to protect them from the effects of engine vibrations. Observations of the failed engine are depicted in Fig. 1. A general view of the engine is shown in Fig. 1 (a) displaying the damage. The assembly mechanism of electric cables and fuel tubes is shown in Fig. 1 (b) and (c). The close-ups in Fig. 1 (b) and (c) indicate the loosened assembly rod bolt and the fractured clip, respectively. During the inspection, it was discovered that a fuel tube connected to the 2.5 master actuator was broken, leading to a significant fuel leak. Additionally, the clip responsible for securing the fuel tube to the engine body had broken, and the nut that was supposed to be fastened to the assembly rod bolt was missing, having detached during flight.

The broken clip, identified as an AS62405 model, features a metallic loop made from AMS 5528 17-7 PH stainless steel with a thickness of 0.6 mm. The failed fuel tube is a seamless 6A5132 model, composed of Fe-18Cr-11Ni-Nb stabilized stainless steel (Type 347 stainless steel), with a diameter of 8 mm and a wall thickness of 1 mm. Both the fractured fuel tube and the broken clip were collected for an in-depth metallurgical analysis to determine the root causes of the failure.

Table 1 Operational history of the damaged engine before the incident.

Total operating time	9854 Hours
Total operating time since last maintenance	2626 Hours
Total cycles	9518 Cycle
Total cycles since last maintenance	3617 Cycle

3. Investigational procedures

The received components were thoroughly investigated using destructive and nondestructive methods. Visual inspection was first conducted on the as-received specimens. A dye penetrant test was applied to the fracture surface according to ISO 3452-1.2021. The chemical compositions of the failed components were analyzed by an optical emission

IJMTI vol. 4 issue 2 (2024) 1-8 https://doi.org/ 10.21608/IJMTI.2024.325019.1108

spectrometer. Microstructure examination was carried out using an optical microscope. Specimens for microstructure examination were cut and prepared as per standard metallographic techniques. The fracture surfaces were investigated using a stereo microscope and a scanning electron microscope (SEM). Hardness measurement was carried out using a Vickers hardness tester with a 1.961 N load and 15 sec dwell time.

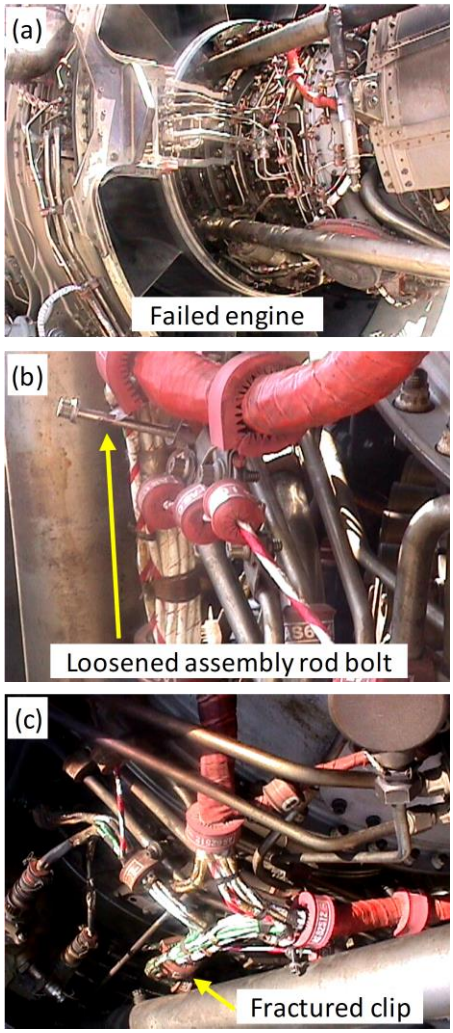

Fig. 1 Damage of the right engine: (a) general view of the engine, (b)close-up of the assembly rod bolt, and (c) close-up of the damaged cable assembly.

4. Results and discussion

4.1 The AS62405 clip

A detailed visual inspection of the fractured AS62405 clip revealed that only one of its terminals had failed, as illustrated in Fig. 2 (a). A general view of an undamaged clip is given in Fig 2 (b) for comparison. Close examination suggested that the fracture initiated from the inner surface of the hole located on the terminal of the broken clip. Despite this fracture, there was no noticeable reduction in the clip's thickness at the fracture site indicating that the structural integrity of the remaining areas of the clip was largely preserved prior to failure. A dye penetrant test was conducted to check for surface cracks, in both the fracture zone and surrounding areas, but no surface cracks were detected.

To gain deeper insight into the failure mechanism, samples were extracted from the broken clip for further analysis. The chemical compositions of the broken clip materials were examined to check their conformity to the standard specifications for AMS 5528 17-7 PH stainless steel. The results are presented in Table 2. The chemical analysis showed that the clip's chemical composition conformed to the specified range for this stainless steel type. This alignment with material specifications suggests that, at least from a compositional standpoint, the clip met the necessary criteria for performance in its intended application.

An optical micrograph depicting the cross-section of the fractured clip is presented in Fig. 3. The microstructural analysis reveals that the material exhibits characteristics consistent with a solution-treated and subsequently reheated condition. The predominant structure comprises a tempered martensite matrix, dispersed with ferrite stringers and carbide precipitates located at the grain boundaries and within the grains themselves. This specific microstructure has been verified by hardness measurements, which yielded an average hardness of 373 HV, consistent with the expected characteristics of tempered martensitic stainless steel.

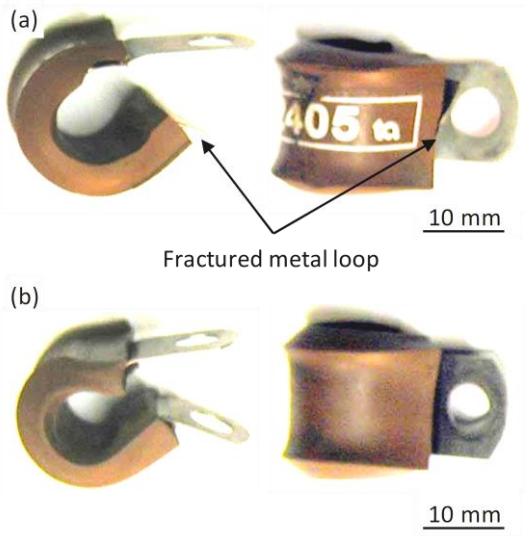

Fig. 2 Photographs of (a) a damaged clip and (b) and an undamaged clip.

IJMTI vol. 4 issue 2 (2024) 1-8 https://doi.org/ 10.21608/IJMTI.2024.325019.1108

Table 2 Chemical compositions of the broken clip material and the standard specifications for AMS 5528 17-7 PH steel, wt.%.

Material	C	Si	Mn	Cr	Ni	Al	Co	Cu	Fe
Broken clip	0.10	0.38	0.58	16.93	8.10	1.5	0.24	0.21	71.9
AMS 5528 17-7 PH steel	0.09 max.	1.00 max.	1.00 max.	16-18	6.5-7.75	0.75- 1.5	….	….	Bal.

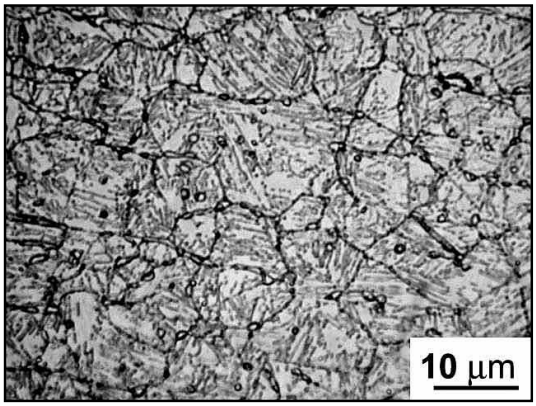

Fig. 3 Microstructure of the broken clip.

A low-magnification stereoscopic image of the fracture surface of the clip is illustrated in Fig. 4 (a). Notably, minimal reduction in thickness was observed across the fractured area. The image highlights a specific zone where the fracture likely initiated—located at the inner surface of the hole in the clip's terminal. This area was marked by a yellow rectangle as the most probable point of fracture initiation.

Further investigation using SEM of the marked fracture initiation zone provided more detailed insights. Radial marks, which are characteristic of fatigue failure, were observed, radiating from the identified initiation point as seen in Fig. 4 (b). These radial markings clearly indicated the direction in which the fracture propagated, as shown by the arrows in Figure 4 (c). Upon examining the fracture surface at higher magnifications, additional evidence of fretting fatigue was detected around the initiation zone, as shown in Fig. 5 (a) and (b). Slip regions characteristic of fretting fatigue were observed and marked by arrows in Fig. 5 (b). Fretting fatigue typically occurs due to small oscillatory movements that create wear and crack initiation under cyclic loading [13].

As the fracture progressed, a transition to a brittle fracture mode was observed near the termination zone of the crack, as displayed in Fig. 5 (c), indicating a change in the failure mechanism as the fracture approached completion. This combination of fatigue and brittle fracture suggests that the clip underwent sustained cyclic loading before ultimately failing in a more abrupt manner.

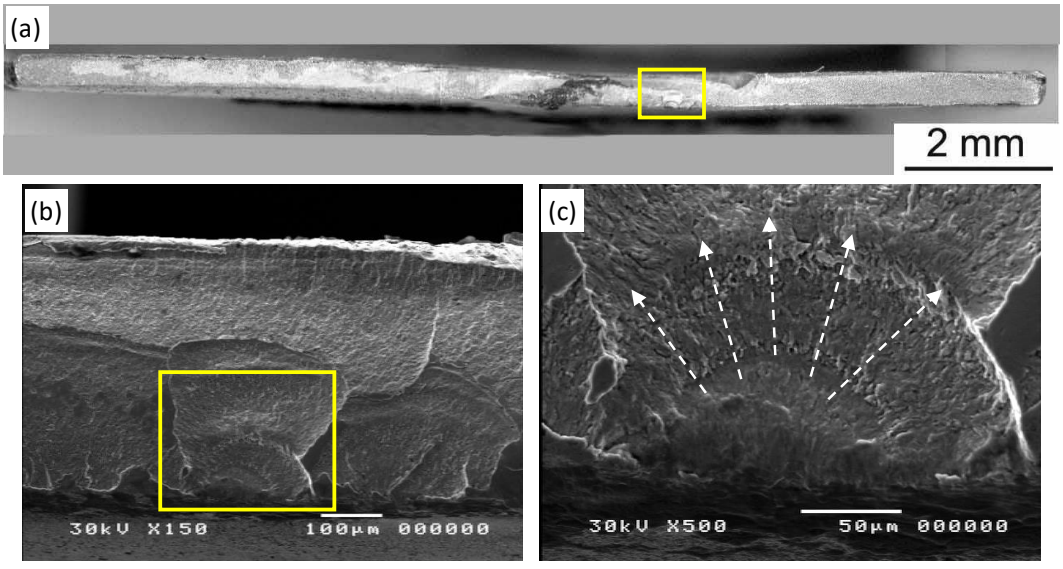

Fig. 4 Fracture surface of the broken clip: (a) Low magnification stereoscopic photograph, (b) a magnified SEM image of the boxed area in (a), and (c) a magnified SEM image of the boxed area in (b).

IJMTI vol. 4 issue 2 (2024) 1-8 https://doi.org/ 10.21608/IJMTI.2024.325019.1108

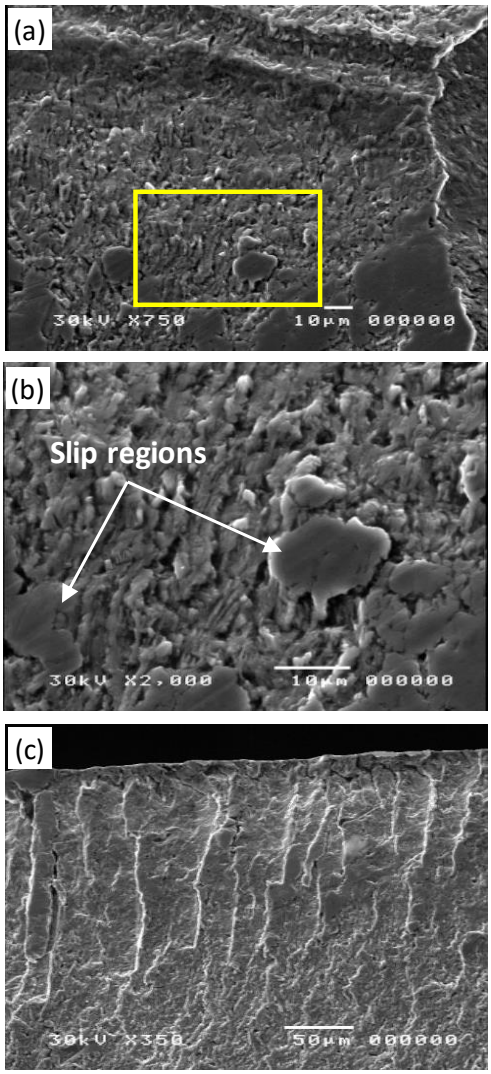

Fig. 5 (a) A SEM image of the clip's fracture surface showing indications for fretting fatigue, (b) a magnified SEM image of the boxed area in (a), and (c) a SEM image at the termination zone of the fracture.

4.2 The 6A5132 fuel tube

A general visual examination of the fractured fuel supply tube assembly is illustrated in Fig. 6 (a), while a detailed view of the fracture zone is presented in Fig. 6 (b). Initial visual inspections indicated that the fuel supply tube had failed, resulting in a separation into two distinct sections, as depicted in Fig. 6 (a). The tube is secured at both ends by inner screw reducers, which are connected through butt-welded joints. Notably, the fracture was located on the tube side of the butt welded joint rather than on the reducer side.

This distinction is critical as it suggests potential weaknesses inherent to the tube material or its connection method. To further investigate the integrity of the fuel supply tube, a dye penetrant test was conducted; this test revealed no surface cracks either in proximity to or distant from the fracture zone, indicating that the failure was not due to pre-existing surface defects. Subsequently, specimens from the fractured tube were extracted and prepared for a series of examinations, including chemical composition analysis, optical and SEM investigations, and hardness testing.

The findings from the chemical analysis of the fractured tube are compared with those of its designated material specifications in Table 3. It was determined that the chemical composition of the fractured tube falls within the acceptable range for type 347 stainless steel, suggesting that material properties were consistent with established standards.

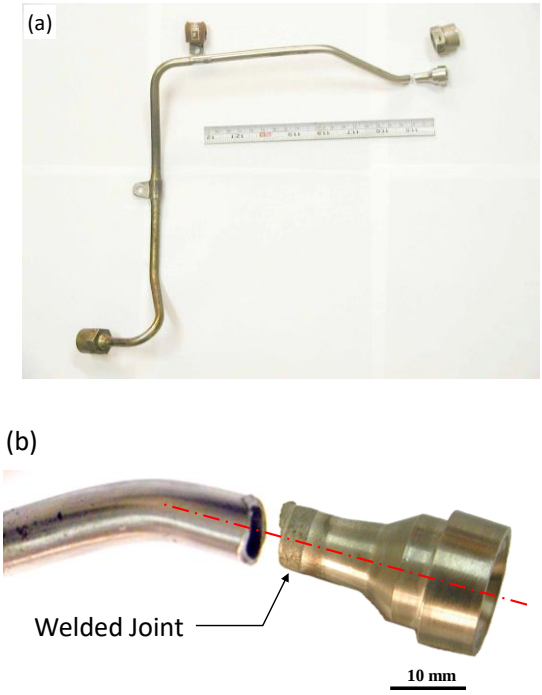

Fig. 6 (a) A general view of the fractured fuel supply tube, and (b) a close-up of the fracture zone.

The fracture surface of the fuel tube, along with longitudinal cross-sections oriented perpendicular to the fracture plane, are depicted in Fig. 7 (a) and (b), respectively. Notably, certain zones of the fracture surface exhibited signs of obliteration due to post-separation rubbing, which may have obscured some features critical for failure analysis.

Importantly, no significant reduction in wall thickness was detected throughout the length of the tube, indicating that the material's structural integrity remained largely intact until the point of failure. The fracture originated within the heat-affected zone (HAZ) of the circumferential butt welded joint, a critical area where thermal influences from welding can alter material properties.

IJMTI vol. 4 issue 2 (2024) 1-8 https://doi.org/ 10.21608/IJMTI.2024.325019.1108

Table 3 Chemical compositions of the fractured tube material and the standard specifications for Type 347 stainless steel, wt.%

Material	C	Si	Mn	Cr	Ni	P	S	Nb	Fe
Fractured tube	0.067	0.285	2.00	17.66	11.05	0.014	0.009	0.60	68.32
347 stainless steel	0.08 max.	1.00 max.	2.00 max.	17-19	9-13	0.045 max.	0.030 max.	10XC min. Nb+Ta	Bal.

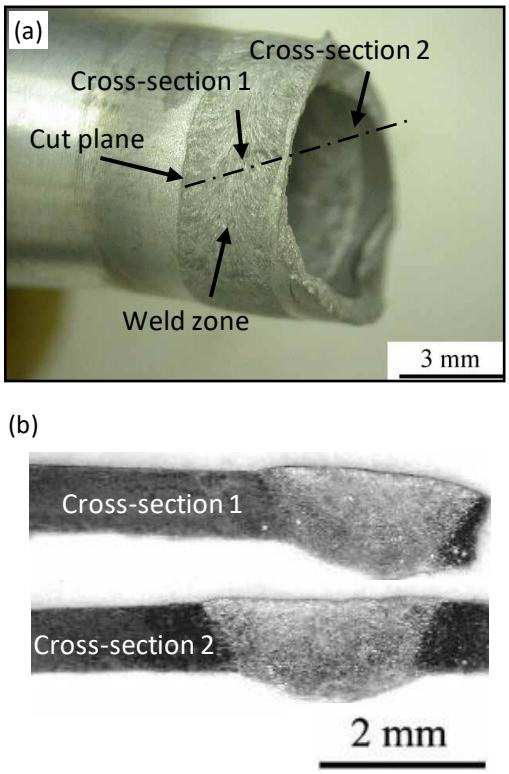

Fig. 7 (a) Fracture zone of the fuel supply tube, and (b) fusion zone macrostructure of the tube circumferential butt welded joint.

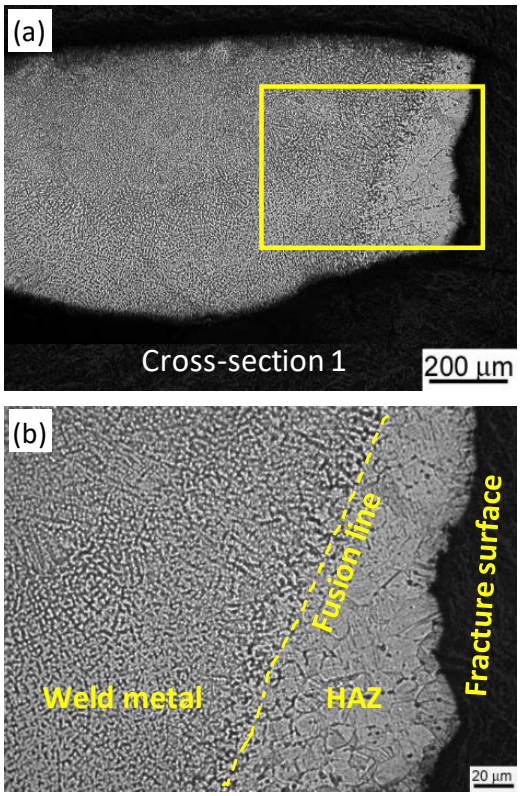

Fig. 8 (a) Microstructure of cross-section 1 in Fig. 7 (b), and (b) a magnified view of the boxed area in (a).

Higher magnification optical micrographs of both the weld metal and the HAZ of cross-section 1 are presented in Fig. 8. These images reveal that the initiation of fracture occurred in the HAZ, very close to the fusion line of the butt weld, and extended into the base metal, indicating a potential weakness in this region. The microstructural analysis confirms that both the weld metal and HAZ display typical austenitic structures characteristic of type 347 stainless steel welded joints. In contrast, the microstructure of the base metal exhibits a non-uniform distribution of austenite grains, dispersed with carbide precipitates along the grain boundaries, as illustrated in Fig. 9. Importantly, no internal defects were identified in any of the examined regions, including the base metal, HAZ, or weld metal. The hardness measurements obtained from

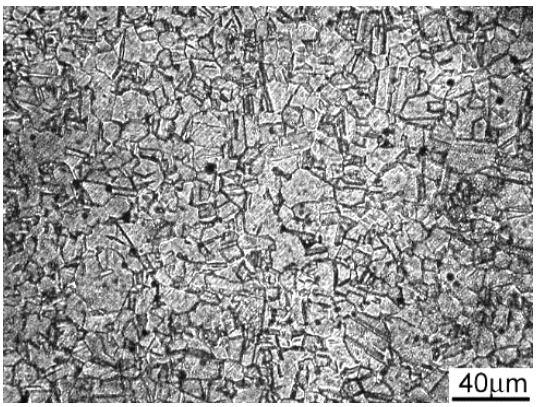

Fig. 9 Base metal microstructure of the fractured fuel tube.

IJMTI vol. 4 issue 2 (2024) 1-8 https://doi.org/ 10.21608/IJMTI.2024.325019.1108

these areas were consistent with expected values: 235 HV for the base metal, 260 HV for the HAZ, and 230 HV for the weld metal, indicating that material properties were within acceptable limits for the base and weld metals, while a relative hardening was observed in the HAZ.

Applying deeper examination using SEM, it was observed that grain boundary cracking initiated at the inner surface of the tube, as seen in Fig. 10 (a). The presence of distinct fatigue striations across various zones of this inner surface suggests that low-cycle fatigue played a significant role in the fracture process, as evidenced by Fig. 10 (b). This observation points to multiple initiation sites contributing to the overall failure mechanism. Additionally, a brittle fracture mode was identified around the termination zone on the outer surface of the tube, as shown in Fig. 11, highlighting a complex synergy between fatigue and brittle failure modes in this incident.

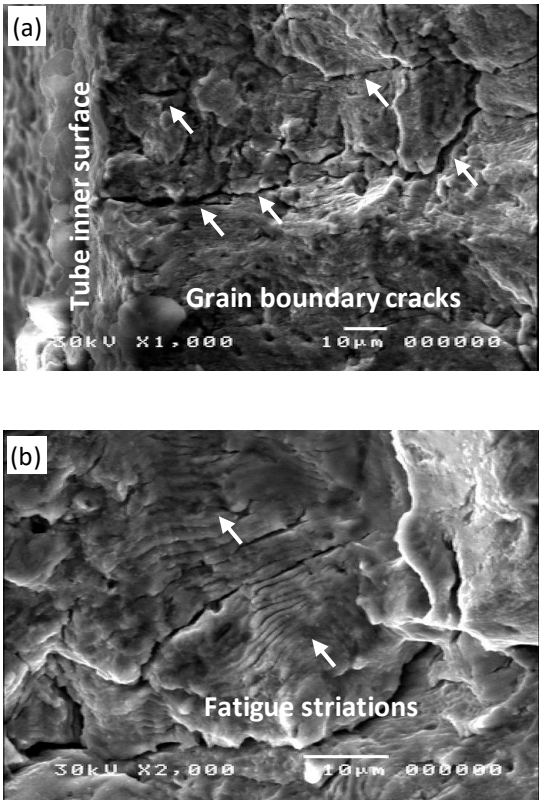

Fig. 10 SEM images of the fuel tube fracture surface showing: (a) grain boundary cracks, and (b) fatigue striations.

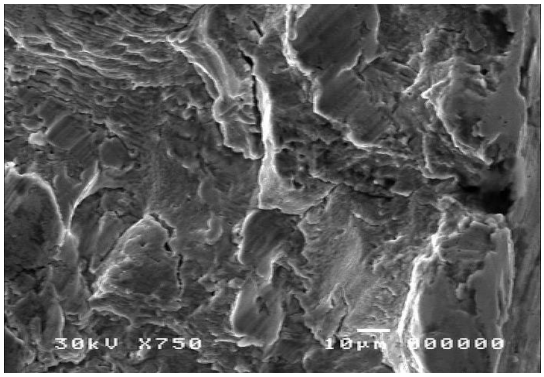

Fig. 11 A SEM image of the fuel tube fracture surface at the crack termination zone.

Conclusions

The analysis indicates that the fracture of the clip was predominantly caused by fretting fatigue. This condition arose from the sliding contact between the surfaces of the fuel tube assembly rod bolt and the clip hole, which experienced minute alternating relative motion due to vibration. Under such fretting conditions, fatigue cracks can initiate at stress levels significantly lower than those typically associated with non-fretted components.

Furthermore, evidence suggests that loosening of the nut securing the assembly rod bolt occurred prior to the ultimate failure of both the clip and the fuel tube. This loosening would have facilitated sliding contact, thereby worsening fretting conditions. It is noteworthy that fatigue strength diminishes as contact pressure increases, indicating that even minor changes in assembly integrity can substantially affect component durability.

The failure of the fuel supply tube is primarily linked to fatigue mechanisms. The loosening of the fuel tube assembly rod bolt, along with the resultant failure of its clip hole, imposed abnormal alternating loads on the fuel tube during engine operation. These atypical vibrational forces likely contributed to fatigue failure. Notably, fatigue cracking was initiated at the inner surface of the tube, particularly in regions characterized by high hardness within the coarse grain HAZ of the butt welded joint.

Acknowledgments

The authors would like to thank all the staff members of the Welding and Inspection Department, CMRDI for their assistance at all stages of this work.

References

[1] Bokwon Lee, Ryan L. Karkkainen, Failure investigation of fuel tubes of a jet engine

augmenter assembly, Eng. Fail. Anal. 62 (2016) 39-48. https://doi.org/10.1016/j.engfailanal.2015.12.003

[2] María Pilar Valles González, Alejandro González Meije, Ana Pastor Muro, María García-Martínez, Beatriz González Caballero, Failure analysis of a fuel control pressure tube from an aircraft engine, Eng. Fail. Anal. 126 (2021) 105452. https://doi.org/10.1016/j.engfailanal.2021.105452

[3] Graham Clark, Failures in military aircraft, Eng. Fail. Anal. 12 (2005) 755-771. https://doi.org/10.1016/j.engfailanal.2004.12.010

[4] Nazir M, Ejaz N, Mansoor M. Vibrational Fatigue of Fuel Pipe Welds of an Aero Engine. Adv. Sci. Technol. 119 (2022) 75–79. https://doi.org/10.4028/p-47qsl4

[5] Bijayani Panda, M. Sujata, M. Madan, K. Raghavendra, S.K. Bhaumik, Fatigue failure of weld joint of afterburner fuel manifold of a jet engine, Eng. Fail. Anal. 30 (2013) 138-146. https://doi.org/10.1016/j.engfailanal.2013.01.022

[6] M. Mansoor, N. Ejaz, Thermal fatigue failure of fuel spray bars of a jet engine afterburner, Eng. Fail. Anal. 18 (2011) 492-498. https://doi.org/10.1016/j.engfailanal.2010.08.003

[7] X. Zhang, D. Wei, S. Yang, Fretting fatigue in dovetail assembly and bridge-flat model: Verification of a life prediction model based on stress gradient, Int. J. Fatigue, 188 (2024) 108500. https://doi.org/10.1016/j.ijfatigue.2024.108500

[8] N. A. Bhatti, M. Abdel Wahab, Fretting fatigue crack nucleation: A review, Tribol. Int. 121 (2018) 121-138. https://doi.org/10.1016/j.triboint.2018.01.029

[9] Y. Kong, C.J. Bennett, C.J. Hyde, A review of non-destructive testing techniques for the in-situ investigation of fretting fatigue cracks, Mater. Des. 196 (2020) 109093. https://doi.org/10.1016/j.matdes.2020.109093

[10] B. Berthel, A.-R. Moustafa, E. Charkaluk, S. Fouvry, Crack nucleation threshold under fretting loading by a thermal method, Tribol. Int. 76 (2014) 35-44. https://doi.org/10.1016/j.triboint.2013.10.008

[11] J. W. Calderón-Hernández, M. Perez-Giraldo, R. Buitrago-Sierra, J. F. Santa-Marín, Failure analysis of loom crankshafts in textile industry by fretting-fatigue, Eng. Fail. Anal. 151 (2023) 107414. https://doi.org/10.1016/j.engfailanal.2023.107414

[12] J. Peng, Y. Zhao, R. Chen, Y. Song, Z. Zhong, J. Liu, Y. Ren, M. Zhu, Study on bending fretting fatigue behaviour of 15-5PH stainless steel with different fretting regimes, Tribol. Int. 194 (2024) 109566. https://doi.org/10.1016/j.triboint.2024.109566

[13] Chowdhury MA, Kowser MdA, Zobaer Shah QMd, Das S. Characteristics and damage mechanisms of bending fretting fatigue of materials, Int. J. Damage Mec. 27 (2018) 453-487. https://doi.org/10.1177/1056789517693412